

3.3.4 LTSK10

Mosaicking Algorithm

A. Algorithm Outline

- (1) Algorithm Code: LTSK 10
- (2) Product Code: L2A_LC
- (3) PI names: G18 Dr. Alfredo Huete
- (4) Overview of algorithm(Standard level)

Algorithm objectives

The algorithm has the following objective:

To mosaic and composite the normalized, at-sensor radiances (apparent reflectance) on 16 day and monthly basis for the 1km and 250m GLI bands (250m bands are processed separately);

- 1,5, 9,13,15,17,19,24,26,27, 28,29 (VIS, NIR, and SWIR bands)
- 30, 31, 34, 35, 36 (MTIR bands)
- 20,21,22,23,28,29 (250m bands)

B. Theoretical Description

(1) Methodology and Logic Flow

A general flowchart describing the mosaicking algorithm is presented in figure 1. At-sensor radiances are radiometrically calibrated at the GAIT processing facility to produce Level-1B data. Cloud detection and screening algorithm (ATSK 1,2 and CTSK1a,b) produces cloud flags on a pixel basis (CLFD_p). Precise geographic registration follows, with the LTSKG algorithm, to produce the Level-1B+CLFD_p gridded 1km resolution. The mosaicking algorithm connects to the data stream at this level (Fig. 1).

The mosaicking (also called compositing) algorithm ingests the gridded Level-1B+cloud mask data and produces the 16-day and monthly surface reflectance composites. The mosaicking algorithm selects the best value over a composite period, based on cloudiness and atmospheric contamination. The constraint view angle maximum value composite (CV-MVC) technique (figure 2) is used to generate these composites. The algorithm works mostly with integer data types, hence requiring less CPU time.

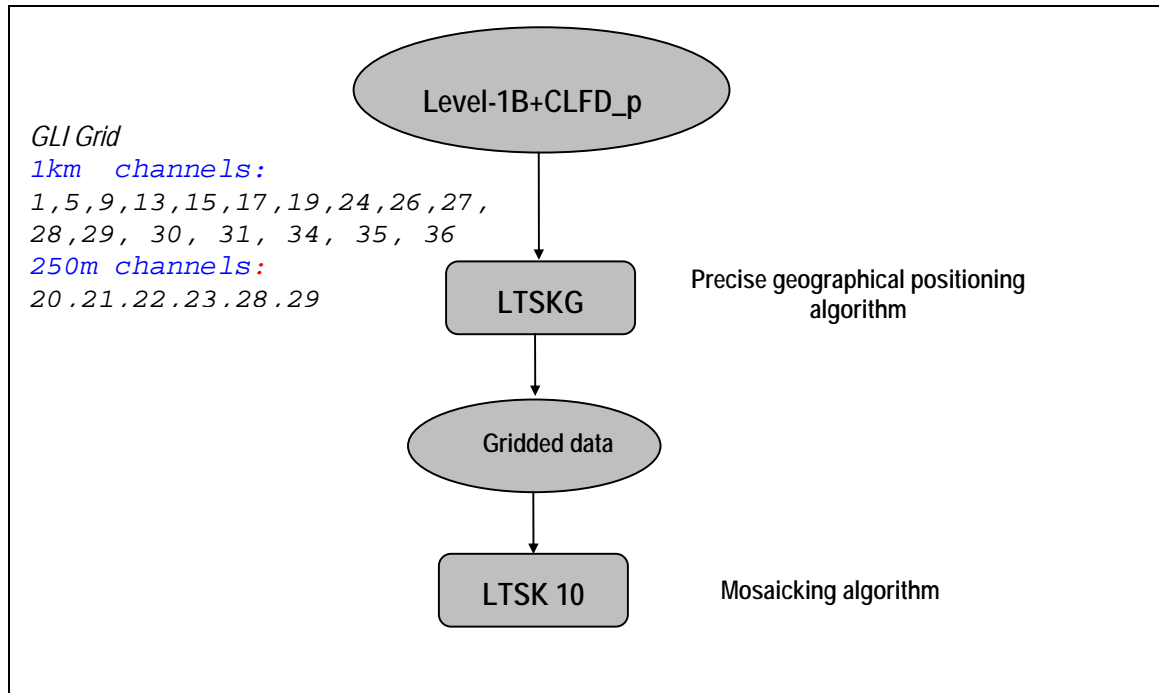


Figure 1: Flow diagram for Mosaicking (LTSK 10)

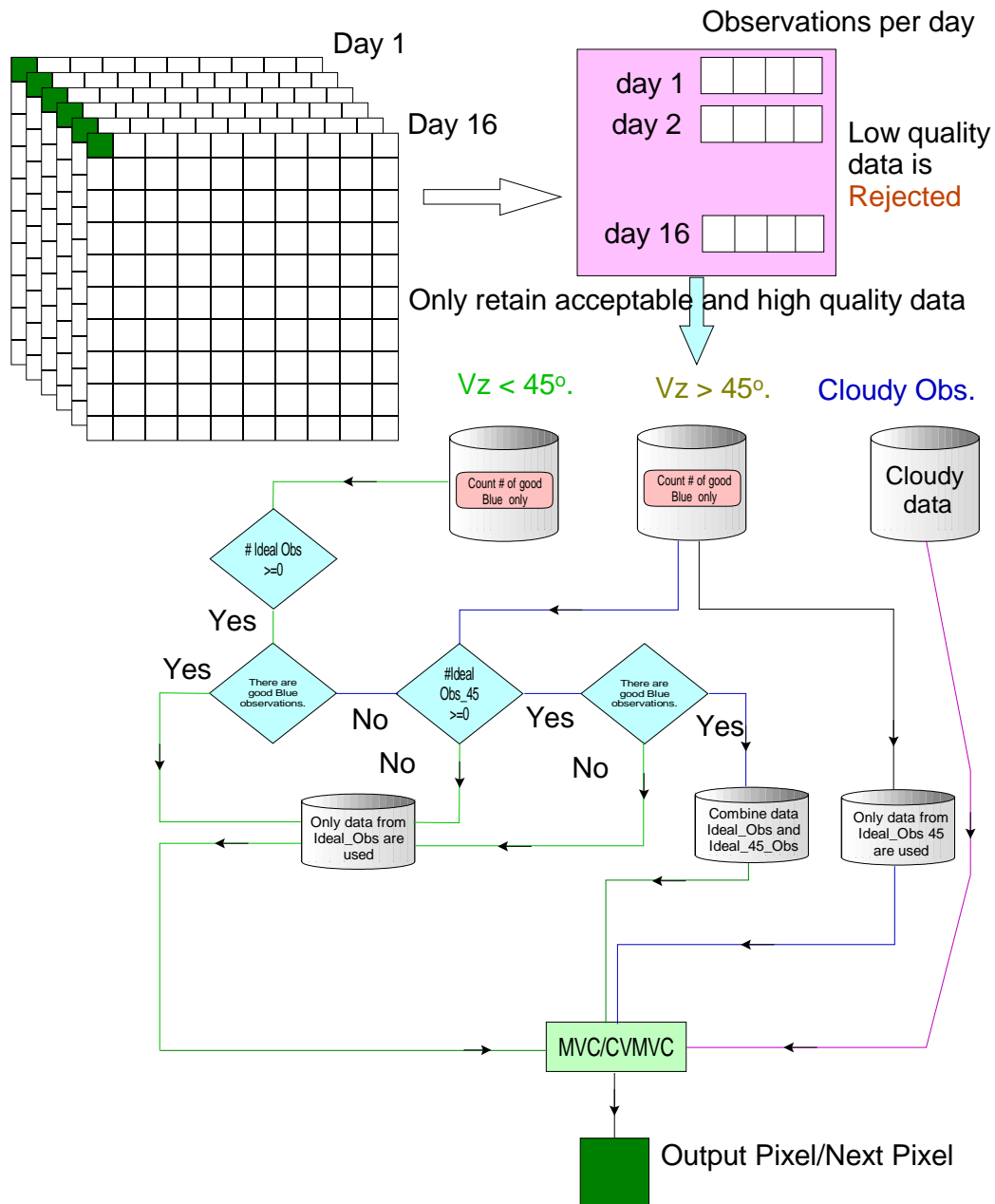


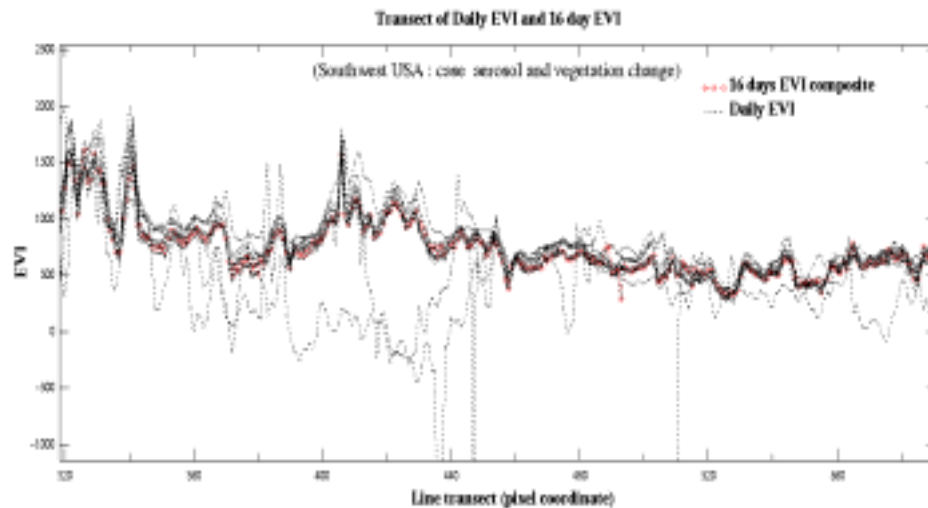
Figure 2: Mosaicking algorithm data flow; Constraint view angle Maximum Value composite

(2) Physical and Mathematical Aspects of the Algorithms

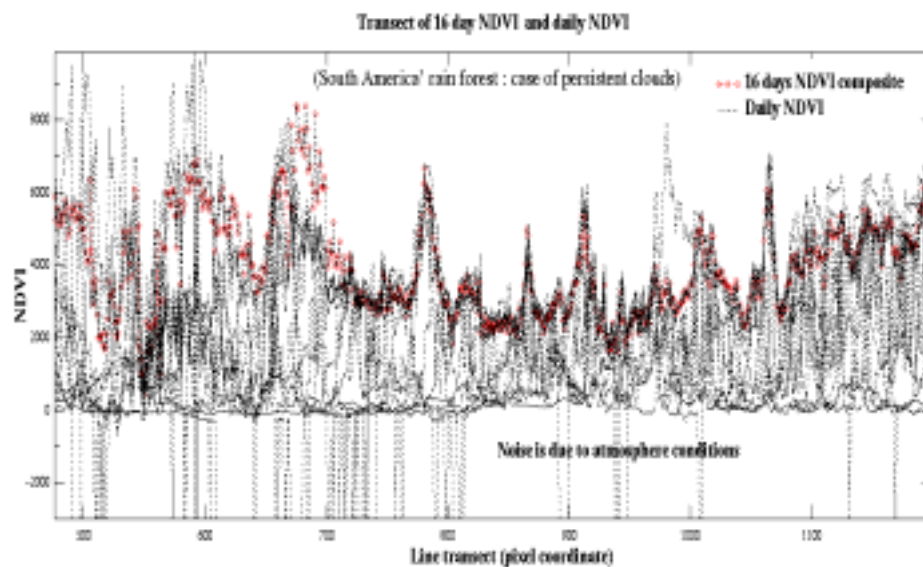
Compositing Algorithm

Although simple in theory, compositing surface reflectance data is a crucial step in producing long-term, stable time series data, to be used in the detection of land surface changes and vegetation dynamics (Tucker et al., 1985, Holben, 1986). In practice, compositing remote

sensing data is complicated owing to the intrinsic behavior of the sensor, surface bi-directional reflectance factors with sun and sensor view angle interactions, and contamination of the spectral response by the presence of residual and persistent clouds, as well as atmospheric aerosols, which are highly variable in space and time (figure 3).



a)



b)

Figure 3a,b: The daily data is very noisy; owing to many factors including clouds, vegetation change over time, viewing geometry. Compositing tries to capture the best possible conditions (minimum cloud, minimum aerosol, best viewing geometry) and generates one value representative of the composite cycle.

Over the composite period, one 'cloud-free' image will be reconstructed out of the temporal period. With GLI four-day global coverage, the sensor will measure every pixel on the earth at least once every four days. With this frequency of observation and the ubiquitous presence of clouds, a practical 16-day compositing period was chosen to match the ADEOS-2 orbital period. Compositing quasi-daily data also entails its reduction to more manageable volumes. Moreover, processing and disk volume limitations mandated the compositing algorithm take place before atmosphere corrections. This scheme fits the research findings and recommendations about the advantages of applying the constraint view maximum value composite (MVC/CV-MVC) on non-atmospherically corrected data (Cihlar et al., 1994a).

2.1 Constraint View Maximum value composite (CV-MVC)

The currently adopted procedure for generation of composited AVHRR-NDVI products is the maximum value composite (MVC) technique (Holben, 1986). The MVC selects the maximum NDVI value on a per pixel basis over a set compositing period and is designed to minimize atmospheric effects, including residual clouds. The compositing procedure generally includes cloud screening and data quality checks (Goward et al., 1994; Eidenshink and Faundeen, 1994).

The MVC works nicely over near-Lambertian surfaces where the primary source of pixel variations within a composite cycle is associated with atmosphere contamination and path length. However, the MVC has problems associated with sun-sensor geometries and surface anisotropies and the maximum NDVI value becomes dependent on both the BRDF properties of the vegetated canopies and varying atmospheric conditions. It tends to overestimate NDVI values by selection of off-nadir pixels in the forward scatter direction resulting in an overestimation of vegetation biophysical parameters. The MVC bias toward selection of off-nadir pixels also results in less accurate atmospheric corrections (longer atmosphere path length). The bi-directional spectral behavior of numerous, "global" land cover types and terrestrial surface conditions have been widely documented and shown to be highly anisotropic due to canopy structure, shadowing, and background contributions (Kimes et al., 1985; van Leeuwen et al., 1994; Vierling et al., 1997). Vegetation indices do not remove surface anisotropy due to BRDF- spectral dependencies with the NIR reflectance response generally more anisotropic than the red reflectance response (Walter-Shea et al., 1997; Gutman, 1991; Roujean et al., 1992).

The MVC approach becomes even less appropriate with atmospherically-corrected data, since the anisotropic behavior of surface reflectances and vegetation indices is stronger (Cihlar et al., 1994b). For these reasons, the MVC method has been found to work best for data uncorrected for atmosphere (Cihlar et al., 1994a), although inconsistencies remain since the MVC favors cloud free pixels, but does not necessarily pick the pixel closest to nadir or with the least atmospheric contamination (Gutman, 1991; Goward et al., 1991, 1994; Cihlar et al., 1994b, 1997). Many studies and experiments have shown the maximum NDVI approach to select pixels with large view and sun angles which are not always cloud-free or atmospherically clear (Goward et al., 1991; Moody and Strahler, 1994; Cihlar et al., 1994b, 1997).

In order to simultaneously remove angular and atmospheric effects from composited

reflectances, both atmosphere and BRDF models are needed. Aerosol retrievals and correction have yet to be implemented on an operational basis. MODIS and MISR will have aerosol corrections but either over much coarser grid sizes or over only limited areas. GLI does not currently plan aerosol correction over land, although there may be some limited areas corrected as the aerosol product over land becomes available. Furthermore, there is no planned BRDF product for the GLI sensor, and this is further complicated by the 4-day repeat coverage, which greatly limits the number of angular measurements from which one could implement a BRDF model.

Our goal with the compositing scheme is to implement an approach that is known to be operational (MVC) with added improvements, which can be shown to be practical with current prototype data sets. One improvement, which is within these goals, is the 'constrained view angle' – MVC, in which the maximum NDVI within a limited range of viewing angles is selected. This is similar to a threshold technique to prevent the selection of extreme off-nadir pixels. Current and ongoing work with MODIS data indicates that in order to reduce the BRDF effects and offset the off-nadir MVC behavior, a simple constraint of the view angle will greatly enhance the results. The constraint view angle (CV-MVC) technique works very much the same way as the classical MVC; After computing the NDVI for each pixel and for each observation the algorithm only retains 'N' pixel with highest NDVI values (N is usually 2 to 4 observations) and chooses the value with the lowest view angle. This will guarantee the elimination of clouds (MVC) and reduces the bias to off-nadir viewing (figure 4).

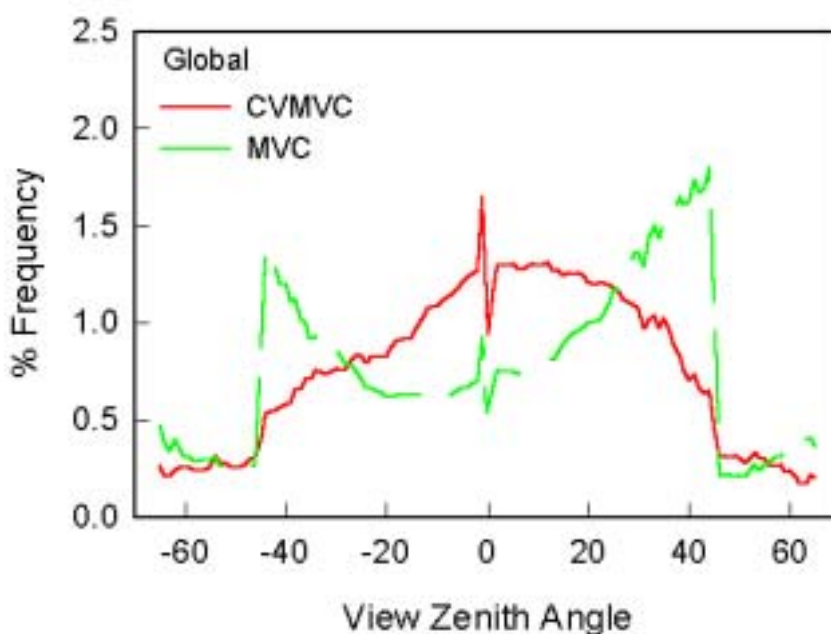


Figure 4: Performance of the CV-MVC and the MVC algorithms. The off-nadir bias is reduced with CV-MVC, (source TBRS non-published research).

We envisage the possibility of post-launch development of additional atmospheric and angular

correction improvements, which are considered experimental at this time. Lastly, we strive to keep the final product as close to the actual measurements as possible so that we may keep track of error and precision and be able to 'validate' the final product.

In summary, the main GLI Vegetation Index compositing goals are to:

- provide accurate and cloud-free vegetation index (VI) imagery at a preset temporal intervals (16 days),
- maximize global and temporal land coverage at the finest spatial and temporal resolutions possible,
- standardize variable sensor view and sun angles,
- ensure the quality and consistency of the composited data,
- depict and reconstruct phenological variations,
- accurately discriminate inter-annual variations in vegetation.

Critical to the quality of the composited vegetation index product will be the co-registration of the different bands used in computing the vegetation indices (red, NIR, and blue), spectral stability of the channels, pixel registration (Townshend et al., 1992) and calibration over time (Price, 1987). Actual day-to-day registration accuracy over a set composite period (16 days) will be determined post-launch.

2.2 Compositing period

Variable composite periods have been used to obtain cloud free NDVI data on a global scale. The minimum compositing period is limited by cloud cover frequency and may vary from every 5 days at higher latitudes to as long as 30 days or more in some humid tropical areas. NDVI composite periods have varied among 7, 9, 10, 11 and 14 days and monthly intervals with variable spatial resolutions (Townshend, 1994). The composite period depends on the final data application and the availability of cloud free data on a global scale. Shorter compositing period will pick up more dynamic land cover changes and allows one to combine compositing periods to monthly or bi-weekly periods. However, the shorter the compositing period, the greater the likelihood of cloud-affected or missing pixels in the composited image. The 16-day period seems appropriate since it gives the possibility to avoid clouds and to cover all latitudes within small viewing angles, providing the best spatial resolution, and the most accurate atmospheric correction. The monthly compositing cycle is based on demand and heritage of the user community. Current work with MODIS (TBRS internal research) indicates that capturing

vegetation change and reducing atmospheric effects on a global basis could be achieved with the 16 days composite period (figure 5).

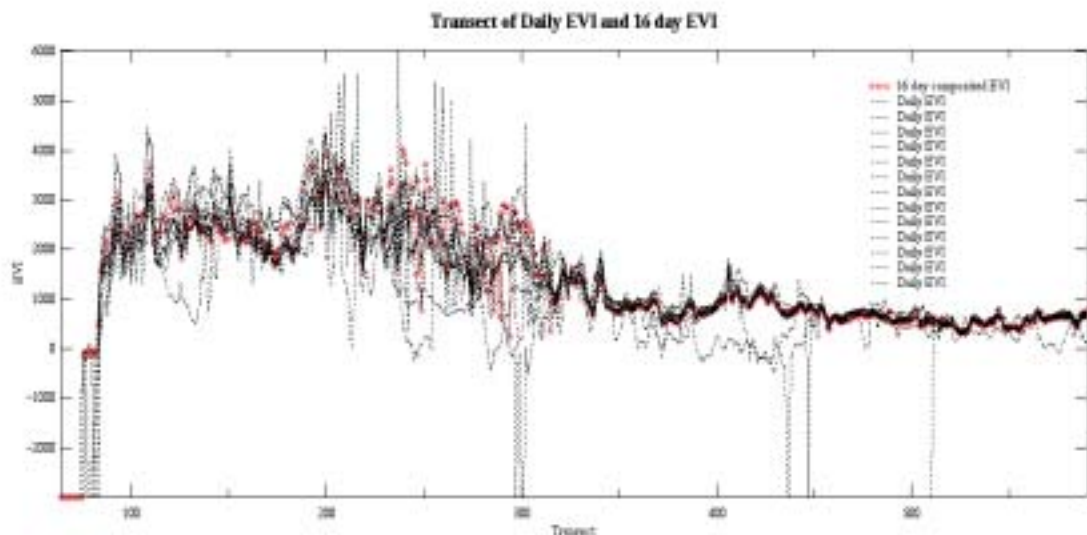


Figure 5: Compositing EVI in relation to the daily EVI, the noise is due to atmosphere conditions, clouds, and viewing geometry and vegetation growth. The 16 days EVI composite captures the vegetation change and reduces this noise.

2.3 GLI data stream

The GLI data stream (calibration of top of the atmosphere (TOA) radiance; cloud mask; land and water mask; mosaicking/compositing; atmospheric correction and surface reflectance; vegetation indices) is set up to flow into the product algorithms in a predetermined order (figure 1). For a tractable and best solution to the compositing algorithm it was logical to use the non-atmospherically corrected reflectance data in combination with the cloud mask as input and use as many "good" observations as possible during a composite period. As depicted in figure 1 and 2, the compositing algorithm processes multi-day gridded data on a pixel basis, for each pixel the MVC/CV-MVC approach is applied and one day (one pixel) is chosen to represent the composite period. The final product of this algorithm will be used to generate the corrected surface reflectance and to compute the vegetation indices.

C. Practical Considerations

In this section we shall explore some of the proposed algorithms aspects with respect to implementation, programming and data interfacing.

(1) Programming, Procedural, Running Considerations

1.1 Compositing Algorithm Implementation

Due to computational limitations (imposed by the GLI production team) we adopted an algorithm scheme as diagrammed in figure 1. We note that atmospheric correction will be posterior to the compositing algorithm, based on the disk and CPU load savings. Reflectance data processed at the GAIT facility and cloud cover from the atmospheric (ATSK algorithms) group will serve as the input for this algorithm. Gridded and tiled Global Coverage Data (GLI land tiles: 1600x1600 km) is processed after precise geographic positioning to generate the composited surface reflectance data. The MVC/ CV-MVC selection criterion is applied to the daily orbits as the data is ingested and compared to previous data. The MVC/ CV-MVC algorithm can be summarized by the next computational steps, on a pixel basis;

Start with current day,

- Ingest pixel (reflectance, location, time, viewing geometry, etc.)
- Apply appropriate land/water and cloud mask
- Check pixel quality
- Pixel passes quality checks
 - Compute NDVI and EVI for the current pixel
 - Assign pixel to current stack (Pixel stack through days)
- Pixel fails
 - Go to next day
- Sort the collected pixels in ascending order by their view zenith angle
 - If MVC is to be applied choose the pixel with the highest NDVI and go to next pixel
 - If CMVC is to be applied, only keep the 2 (3 or 4) pixels with lowest view zenith
- Choose from the above list the pixel with the highest NDVI
- Go to next pixel

Due to the temporal resolution of GLI (4 days at the equator), each pixel will be reproduced approximately once every four days, and multiple observations for the same day due to the orbital overlap. During a compositing period (16 days) at least one out the four or more pixels will be chosen. Moreover, due to some of the problems reported with MVC off-nadir pixel selection, a CV-MVC approach can be used when a ‘run time flag’ is specified (See code: LTSK_10_Composite.c). The CV-MVC, will try to limit the processing to only the pixels with a view angle close to nadir. Figure 6 illustrates the steps required to conduct an effective MVC/CV-MVC. In order to reduced computational load, GAC data will be processed in multiple lines and stored into the final composite image.

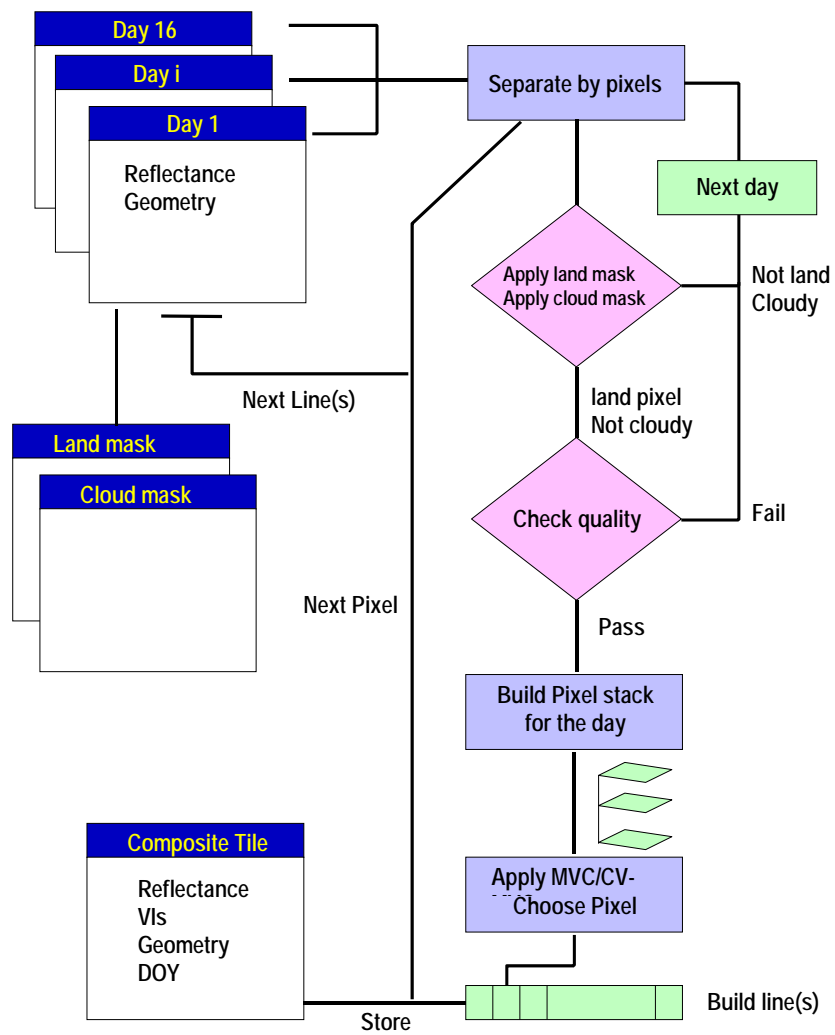


Figure 6. MVC/CV-MVC Algorithm data flow

1.2 Numerical and computation considerations

GAIT requires that all GLI production algorithms be modular and written in C, or FORTRAN (ANSI). All data types (input and output) are in short integer format. For accuracy reasons the reflectance data will be scaled to 10,000 and vegetation index computation will be carried in floating point format. As with any other project of this magnitude, a sound system of input/output specification is devised to optimize algorithm performance and reduce processing requirements. A data structure is used to record the different characteristics of a pixel as it is processed at the different stages (location, date, viewing angles, geometric angles, cloud cover, etc.). This data structure generated at LTSKG algorithm level is built upon to accommodate attributes required by or generated by subsequent algorithms. Overall, this structure is updated by the processing algorithm discarding redundant data based on downstream algorithm requirement. The final product is stored in the HDF files (Hierarchical Data Format), which is widely adopted by the remote sensing community. Developed to be self-describing and portable format, the HDF will allow data sharing between the different algorithms without the need to describe it. Description data (called meta-data) will be stored with every layer of information to provide accurate and efficient exchange.

As part of the algorithm implementation, each pixel will have a set QA/QC flags that reflect the data quality and capture processing and ingestion problems. Various other attributes can be added to the above format if required by the higher order GLI algorithms and products.

(2) Calibration and Validation

(3) Quality Control and Diagnostic Information

Once proper attributes are present, the LTSK 1 algorithm will execute and replace the normalized apparent reflectances (generated by LTSK 9) with the atmospherically corrected reflectances. Both LTSK 1 and LTSK 9 outputs are temporary, but the use of quality assurance and quality control flags assures the proper interfacing between the science parts of the algorithms. The algorithm generates diagnostics messages that capture production errors and the required actions to correct them.

(4) Exception Handling

Exception handling is the technique of accounting for unforeseen situations. Missing data, missing ancillary data, floating point error during computation, data out of range, should be

all properly ingested and documented during the run. In a generic approach, any time the algorithm does not perform as designed, the code will generate an exception handler to be processed separately by the algorithm. During the run the algorithm uses a success flag to track the execution of the different parts. Anytime an exception handler is generated the pixel value will not be updated and a pre-determined fill-value (-3000, -2000, etc...) will be appended instead. All pixels will contain data at the end of the process, and the user will be able to identify the bad pixel by the presence of fill values along with QA/QC flags.

(5) Constraints, Limitations, Assumptions

As proposed in phase one, we implemented an MVC/CV-MVC compositing algorithm that operates on uncorrected surface reflectance. This compositing algorithm has some constraint and assumptions:

- Does not account for surface reflectance angular dependencies (BRDF)
- Assumes the cloud-screening algorithm performs well. Cloud flags are used to filter data prior to compositing, hence their accuracies are crucial.
- Day to day accurate geolocation and registration is crucial to the compositing, usually quarter to half a pixel error is acceptable
- Band to band registration is another issue to be analyzed post launch

Because of the number (18 bands) and spectral nature of bands (VIS, NIR, SWIR, and Thermal) used during the compositing, the resulting product is only optimized for vegetation index generation. Composited thermal band in this case is not an accurate product, rather it only represents a by-product of compositing land bands (red, NIR, and blue). Other bands might suffer from the same problem too, due to their spectral location. Hence, it is crucial to realize that this product is based on optimizing the land bands, and only bands used in computing the vegetation index. All other bands are only kept in the data set and are by no means properly composited. Other techniques for compositing thermal bands exist but not used here due to the nature and goals of the algorithm. The same problem is also noted when performing atmosphere correction, L2A_1 (atmosphere correction algorithm) is designed to work better with the land channels, and it only performs Rayleigh and Ozone correction, which are not appropriate for thermal bands. The presence of 18 bands in the composite product (L2A_LC) is the

result of a GAIT requirement that aimed at making them available for downstream products.

(6) Suggestions and Recommendations

Our involvement with the MODIS project helped us learn more about the performance of the MVC/CV-MVC compositing algorithm. For instance, analysis of the MODIS compositing algorithm indicates that the CV-MVC is superior to the classical and simple MVC. Moreover, the GLI adoption of compositing normalized surface reflectance, rather than corrected reflectance, will serve two goals:

- Reduced CPU and disk space requirements, by means of only correcting the data once every composite period (once every 16 days) as opposed to every day (case of MODIS).
- MVC and subsequently CV-MVC is shown to perform better when performed on non-atmospherically corrected data.

Our main suggestions are to separate between the land and thermal bands compositing. Compositing thermal bands with MVC/CV-MVC is not the proper scheme, and will only result in their misappropriate interpretation. Actually this separation can farther reduce the CPU and disk usage.

As explained in previous GLI report, a wealth of SeaWiFS data was acquired by our group for the purpose of testing and prototyping the GLI algorithms. We aimed at thoroughly establishing the soundness of our atmosphere correction and vegetation index compositing strategies. As stated above, both MVC and CV-MVC along with a generic cloud mask were carried with success, we were able to generate global VI prototypes under different scenario. Moreover, the availability of MODIS data (since April 2000) made it possible to further test and prototype our algorithm. The current MVC/CV-MVC performed well either with a cloud mask or not. We caution however, that the presence of a cloud mask is critical to the application of an MVC/CV-MVC scheme. The algorithm is flexible enough with respect to data structure, number of bands (which could be reduced) and the size of the spatial units (tiles), it performed very well when tested with AVHRR, SeaWiFS and currently with MODIS data.

D. References

Ackerman, S., K. Strabala, P. Menzies, R. Frey, C. Moeller, L. Gumley, B. Baum, C. Schaaf, G. Riggs, R. Welch, 1996. Discriminating Clear-sky from Cloud with Modis Algorithm Theoretical Basis Document V3,

<http://eosps0.gsfc.nasa.gov/atbd/modistables.html>.

- Agbu, P.A., and James, M.E., 1994. The NOAA/NASA Pathfinder AVHRR Land Data Set User's Manual. Goddard Distributed Active Archive Center, NASA, Goddard Space Flight Center, Greenbelt.
- Asano, S. and Uchiyama, A. (1987), Application of an extended ESFT method to calculation of solar heating rates by water vapor absorption, *J. Quant. Spectrosc. Radiat. Transfer*, 38. 147-158.
- Asrar, G., Fuchs, M., Kanemasu, E.T. and Hatfield, J.L., 1984, Estimating absorbed photosynthetic radiation and leaf area index from spectral reflectance in wheat, *Agron. J.*, 76:300—306.
- Asrar, G., Myneni, R.B., and Choudhury, B.J., 1992, Spatial heterogeneity in vegetation canopies and remote sensing of absorbed photosynthetically active radiation: a modeling study. *Remote Sens. Environ.* 41:85-101.
- Baret, F., and Guyot, G., 1991. Potentials and limits of vegetation indices for LAI and APAR assessment. *Remote Sens. Environ.* 35: 161-173.
- Bohren, C.F. and Huffman, D.R. (1983), *Absorption and Scattering of Light by Small Particles*, Wiley-Interscience, New York.
- Chandrasekhar, S. (1960), *Radiative Transfer*, Dover, New York. Coulson, K.L., (1988) *Polarization and Intensity of Light in the Atmosphere*, A. Deepak, Hampton, Virginia.
- Choudhury, B.J., 1987, Relationships between vegetation indices, radiation absorption, and net photosynthesis evaluated by a sensitivity analysis, *Remote Sens. Environ.* 22:209-233.
- Cihlar, J., Manak, D., and D'Orio, M., 1994b. Evaluation of Compositing Algorithms for AVHRR Data over Land. *IEEE Trans. Geosc. Remote Sens.*, 32:427-437.
- Cihlar, J., Manak, D., and Voisin, N., 1994a. AVHRR Bidirectional Reflectance Effects and Compositing. *Remote Sens. Environ.*, 48:77-88
- Cihlar, J.C., H. Ly, Z. Li, J. Chen, H. Pokrant, and F. Huang, 1997. Multitemporal, Multichannel AVHRR data sets for Land Biosphere Studies— Artifacts and Corrections. *Remote Sens. Environ.* 60:35-57.
- Deering, D.W. and Eck, T.E., 1987. Atmospheric optical depth effects on angular anisotropy of plant canopy reflectance. *Int. J. Remote Sensing*, 8(6), 893-916.
- Deering, D.W. and Leone, 1986. A sphere-scanning radiometer for rapid directional measurements of sky and ground radiance, *Remote Sens. Environ.*, 19:1-24.
- Eidenshink, J.C. and Faundeen, J.L., 1994, "The 1km AVHRR global land data set: first stages in implementation," *Int. J. Remote Sensing*, 15(17), pp. 3443-3462.
- Fung, Y., Tucker, C.J. and Prentice, K.C., 1987. Application of Advanced Very High Resolution Radiometer Vegetation Index to Study Atmosphere-Biosphere Exchange of CO₂. *J. Geoph. Res.*, 92, 2999-3015.
- Giver, L.P., Benner, D.C., Tomasko, M.G., Fink, U. and Kerola, D.X. (1990), Gaussian quadrature exponential sum modeling of near infrared methane laboratory spectra obtained at temperatures from 106 to 297 K., in *First International Conference on Laboratory Research for Planetary Atmospheres*, pp. 147-156. NASA CP 3077.
- Goody, R.M. and Yung, Y.L. (1989), *Atmospheric Radiation: Theoretical Basis*, Second Edition, Oxford University Press, New York.
- Gordon, H.R., Brown, J.W., and Evans, R. H. (1988), Exact Rayleigh scattering calculations for use with the Nimbus-7 Coastal Zone Color Scanner, *Applied Optics*, 27, 862-871.
- Goward, D.G., Turner, S., Dye, D.G., and Liang, J., 1994. University of Maryland improved Global Vegetation Index. *Int. J. Remote Sensing*, 15(17), 3365-3395.
- Goward, S.N. Dye, D.G., Turner, S., and Yang, J., 1993. Objective assessment of the NOAA global vegetation index data product. *Int. J. Remote Sensing*, 14, 3365-3394.
- Goward, S.N., and Huemmrich, K.F., 1992, Vegetation canopy PAR absorptance and the normalized difference vegetation index: an assessment using the SAIL model, *Remote Sens. Environ.* 39:119-140.
- Goward, S.N., B. Markham, D.G. Dye, W. Dulaney, J. Yang, 1991, "Normalized difference vegetation index

- measurements from the Advanced Very High Resolution Radiometer”, *Remote Sens. Environ.*, 35:257-277.
- Gutman, G.G., 1991, Vegetation indices from AVHRR: an update and future prospect, *Remote Sens. Environ.*, 35:121-136
- Hansen, J.E. (1971), Multiple scattering of polarized light in planetary atmospheres. Part II. Sunlight reflected by terrestrial water clouds, *J. Atmos. Sci.*, 28, 1400-1426.
- Hansen, J.E. and Travis, L.D. (1974), Light scattering in planetary atmospheres, *Space Sci. Rev.*, 16, 527-610.
- Herman, B.M. and Browning, S.R. (1965), A numerical solution to the equation of radiative transfer, *J. Atmos. Sci.*, 22, 559-566.
- Holben, B.N. 1986. Characterization of maximum value composites from temporal AVHRR data. *Int. J. Remote Sensing*, 7:1417-1434.
- Huete, A.R., 1988, A soil adjusted vegetation index (SAVI), *Remote Sens. Environ.* 25:295-309.
- Huete, A.R., Justice, C.O., van Leeuwen, W.J.D., 1996. “MODIS vegetation Index, Algorithm Theoretical Basis Document,” <http://eospsa.gsfc.nasa.gov/atbd/modistables.html>.
- Huete, A.R., Liu, H.Q., Batchily, K., and van Leeuwen, W., 1997, A comparison of vegetation indices over a global set of TM images for EOS-MODIS, *Remote Sens. Environ.*, 59:440-451.
- Iqbal, M. (1983), *Introduction to Solar Radiation*, Academic Press, New York.
- James, M.D., and Kalluri, S.N.V. (1994), The Pathfinder AVHRR land data set: An improved coarse resolution data set for terrestrial monitoring, *Int. J. Remote Sensing*, 15(17):3347-3363.
- Justice, C.O., Townshend, J.R.G., Holben, B.N. and Tucker, C.J., 1985, “Analysis of the phenology of global vegetation using meteorological satellite data”, *Int. J. Remote Sensing*, 6:1271-1318.
- Kaufman, Y.J. and Tanré, D., 1992, Atmospherically resistant vegetation index (ARVI) for EOS-MODIS, *IEEE Trans. Geosci. Remote Sensing*, 30:261-270.
- Kerola, D. X. (1994), *Near-Infrared Spectroscopic Studies of the Troposphere of Saturn*, Ph.D. Dissertation The University of Arizona.
- Kerola, D. X. (1996), Polarization and intensity of sunlight in the Earth's atmosphere: revisiting the Gauss-Seidel modeling approach, *Bull. Amer. Astron. Soc.*, 28, 1158.
- Kerola, D. X., Larson, H. P., and Tomasko, M. G. (1997), Analysis of the near-IR spectrum of Saturn: a comprehensive radiative transfer model of its middle and upper troposphere, *Icarus*, 127, 190-212.
- Kimes, D.S., Holben, B.N., Tucker, C.J., and Newcomb, W.W., 1984. Optimal directional view angles for remote-sensing missions. *Int. J. Remote Sensing* 5(6), 887-908.
- Kimes, D.S., Newcomb, N.W., Tucker, C.J., Zonneveld, I.S., Van Wijngaarden, W. De Leeuw, J. and Epema, G.F. (1985), Directional reflectance factor distributions for cover types of northern Africa, *Remote Sens. Environ.*, 17, 1-19.
- Kimes, D.S., Newcomb, W.W., Tucker, C.J., Zonneveld, I.S., Van Wijngaarden, W., De Leeuw, J., and Epema, G.F., 1985. Directional Reflectance Factor Distribution for Cover Types of Northern Africa. *Remote Sens. Environ.* 18:1-19.
- Kuchler, A.W., 1995. Natural vegetation map, In: Rand McNally Goode's World Atlas; 19th edition. Eds. Espenshade E.B. Hudson, J.C., Morrison, J.L.. p 18-19.
- Lacis, A. (1990), private communication. Leckner, B. (1978), The spectral distribution of solar radiation at the earth's surface - elements of a model, *Solar Energy*, 20(2), 143-150.
- Leeuwen van, W.J.D. A.R. Huete, S. Jia, C.L. Walthall, 1996. Comparison of Vegetation Index Compositing Scenarios: BRDF Versus Maximum VI Approaches. *IEEE- IGARSS'96, Lincoln Nebraska, Vol.3*, 1423-1425.
- Leeuwen van, W.J.D., A.R. Huete, J. Duncan, J. Franklin, 1994. Radiative transfer in shrub savanna sites in Niger -- preliminary results from HAPEX-II-Sahel: 3. Optical dynamics and vegetation index sensitivity to biomass and plant cover. *Agricultural and Forest Meteorology* 69, 267-288.

- Leeuwen van, W.J.D., A.R. Huete., K. Didan and T. Laing, 1997a. Modeling bi-directional reflectance factors for different land cover types and surface components to standardize vegetation indices. 7th Int. Symp. Phys. Measurements and Signatures in Remote Sensing, Courcheval. (pp 1-8; in press)
- Leeuwen van, W.J.D., Trevor W. Laing, and Alfredo R. Huete, 1997b. Quality Assurance of Global Vegetation Index Compositing Algorithms Using AVHRR Data. IEEE- IGARSS'97, Singapore (pp 1-3; in press)
- Liou, K.N. (1980), An Introduction to Atmospheric Radiation, Academic Press, San Diego.
- Liu, H.Q., and Huete, A.R., 1995, "A feedback based modification of the NDVI to minimize canopy background and atmospheric noise", IEEE Trans. Geosci. Remote Sensing, 33:457-465.
- Marchuk, G.I. (1980), The Monte Carlo Methods in Atmospheric Optics, Springer-Verlag, New York.
- Mercer, R.D., Dunkelmann, L., Shaw, G. E., Larson, S. M. and Kerola, D. X. (1997), Solar spectral radiance measurements: connectivity across time and place, Proceedings of the NEWRAD'97 conference, held in Tucson, Arizona, October 27-29, 1997.
- Meyer, D., Verstraete, M. and Pinty, B., 1995. The effect of surface anisotropy and viewing geometry on the estimation of NDVI from AVHRR. Remote Sensing Reviews, 12:3-27.
- Miura T., A. Huete, van Leeuwen. W.J.D., K. Didan, 1997. Vegetation Detection Through Smoke Filled AVIRIS images: An assessment using MODIS band passes. J. Geoph. Res.. Submitted
- Moody, A. and Strahler, A.H., 1994, Characteristics of composited AVHRR data and problems in their classification. Int. J. Remote Sensing, 15(17), 3473-3491.
- Myneni, R.B. and Asrar, G., 1993, Atmospheric effects and spectral vegetation indices, Remote Sens. Environ.
- Myneni, R.B., Hall, F.G., Sellers, P.J., and Marshak, A.L., 1995, "The interpretation of spectral vegetation indices", IEEE Trans. Geosci. Remote Sens.
- Nemani, R., Pierce, L., Running, S., and Band, L., 1993. Forest ecosystem processes at the watershed scale: sensitivity to remotely-sensed Leaf Area Index estimates. Int. J. Remote Sens. 14(13): 2519-2534.
- Price, J.C., 1987. Calibration of Satellite Radiometers and the Comparison of Vegetation Indices. Rem. Sensing Environ., 21:419-422.
- Prince, S.D., 1991, A model of regional primary production for use with coarse resolution satellite data. International Journal of Remote Sensing, 12(6):1313-1330.
- Privette, J.L. Myneni, R.B., Emery, W.J. and Hall, F.G., 1996a. Optimal sampling conditions for estimating grassland parameters via reflectance model inversions. IEEE Trans. Geosci. Remote Sens. Vol. 34(1):272-284.
- Privette, J.L., Deering, D.W., and Eck, T.E., 1996b. Estimating albedo and nadir reflectance through inversion of simple BRDF models with AVHRR/MODIS-like data. J. Geoph. Res. BOREAS special issue, submitted.
- Qi, J. and Kerr, Y., 1997. On Current Compositing Algorithms. Remote Sensing Reviews, 15:235-256.
- Qi, J., Huete, A.R., Hood, J., and Kerr, Y., 1994c. Compositing Multi-temporal remote sensing data sets. PECORA 11, Symposium on land information systems, Sioux Falls August 1993. p. 206-213.
- Rahman, H., Pinty, B. and Verstraete, M.M., 1993. Coupled surface-atmosphere reflectance (CSAR) model 2. Semi-empirical surface model usable with NOAA AVHRR. J. Geophys. Res. 89(D11):20791-20801.
- Raich, J.W., and Schlesinger, W.H., 1992, The global carbon dioxide flux in soil respiration and its relationship to vegetation and climate, Tellus 44B:81-99.
- Roujean, J.L., Leroy, M., Podaire, A., and Deschamps, P.Y., 1992. Evidence of surface reflectance bidirectional effects from a NOAA/AVHRR multi-temporal data set. Int. J. Remote Sensing 13(4), 685-698.
- Roy, D.P., 1997. Investigation of the maximum normalized difference Vegetation Index (NDVI) and the Maximum surface temperature (T_s) AVHRR compositing procedures for the extraction of NDVI and T_s over forest. Int. J. Remote Sens. 18(11):2383-2401.
- Running, S.W., and Nemani, R.R, 1988, Relating seasonal patterns of the AVHRR vegetation index to simulated

- photosynthesis and transpiration of forest in different climates, *Remote Sens. Environ.* 24:347-367.
- Running, S.W., Justice, C., Salomonson, V., Hall, D., Barker, J., Kaufmann, Y., Strahler, A., Huete, A., Muller, J.P., VanderBilt, V., Wan, Z.M., Teillet, P. and Carneggie, D., 1994. Terrestrial Remote Sensing Science and Algorithms planned for EOS/MODIS. *Int. J. Remote Sensing*, Vol. 15, 17:3587-3620.
- Salomonson, V.V., Barnes, W.L., Maymon, P.W., Montgomery, H.E. and Ostrow, H., 1989, MODIS: advanced facility instrument for studies of the earth as a system, *IEEE Trans. Geosci. Remote Sens.* 27:145-153.
- Sellers, P.C. , 1985, Canopy Reflectance, photosynthesis and transpiration, *Int. J. Remote Sens.* 6:1335-1372
- Sellers, P.J., Tucker, C.J., Collatz, G.J., Los S., Justice, C.O., Dazlich, D.A., and Randall, D.A., 1994, "A global 1° * 1° NDVI data set for climate studies. Part 2 - The adjustment of the NDVI and generation of global fields of terrestrial biophysical parameters", *Int. J. Remote Sensing*, 15:3519-3545.
- Stowe, L.L., E.P. McClain, R. Carey, P. Pellegrino, G.G. Gutman, P. Davis, C. Long, and S. Hart. 1991. Global distribution of cloud cover derived from NOAA/AVHRR operational satellite data. *Advances in Space Research*, 3:51-54.
- Strahler, A, et al., 1996. MODIS BRDF/Albedo Product : ATBD version 4. <http://eosps.gsfc.nasa.gov/atbd/modistables.html>.
- Tans, P.P., Fung, I.Y., and Takahashi, T. (1990), Observational constraints on the global atmosphere CO2 budget. *Science* 247:1431-1438.
- Teillet, P.M., Staenz, K., and Willams, D.J., 1997. Effects of Spectral, Spatial , and Radiometric Characteristics on Remote Sensing Vegetation Indices of Forested Regions. *Remote Sens. Environ.* 61:139-149.
- Thome, K.J., Gellman, D.I., Parada, R.J., Biggar, S.F., Slater, P.N., and Moran, M.S. (1993), In-flight radiometric calibration of Landsat-5 Thematic Mapper from 1984 to present, in *Proceedings of SPIE*, vol. 1938, 126-130.
- Tomasko, M.G. and Doose, L.R. (1989), private communication.
- Townshend, J.R.G., 1994, Global data sets for land applications from the AVHRR: an introduction. *Int. J. Remote Sensing*, 15:3319-3332.
- Townshend, J.R.G., C. Justice, W. Li, C. Gurney, and J. McManus, 1991, "Global land cover classification by remote sensing: present capabilities and future possibilities", *Remote Sens. Environ.*, 35:243-256.
- Townshend, J.R.G., Justice, C.O., Gurney, C. and McManus, J., 1992, The impact of misregistration on the detection of changes in land cover, *IEEE Trans. Geosci. Remote Sens.*, 30(5):1054-1060.
- Tucker, C.J. and Sellers, P.J., 1986, Satellite remote sensing of primary productivity, *International Journal of Remote Sensing*, 7:1395-1416.
- Vermote, E., Remer, L.A., Justice, C.O., Kaufman, Y.J., and Tanré, 1995, ATBD Atmosphere correction algorithm: Spectral reflectances (MOD09), Version 2.
- Vermote, E., Tanré, D., Deuzé, J.L., Herman, M., and Mockette, J.J., 1997, Second Simulation of the Satellite Signal in the Solar Spectrum: an overview. *IEEE Trans. Geosc. Remote Sens.*, 35(3):675-686.
- Vermote, E.F., Tanre, D., Deuze, J.L., Herman, M. and Morcrette, J.J. (1997), Second simulation of the satellite signal in the solar spectrum, 6S: an overview, *IEEE Transactions on Geoscience and Remote Sensing*, 35, No. 3, 675-686.
- Vierling, L.A., Deering, D.W., Eck, T.F., 1997. Differences in Arctic Tundra Vegetation Type and Phenology as Seen Using Bidirectional Radiometry in the Early Growing Season. *Remote Sens. Environ.* 60:71-82.
- Viovy, N., Arino, O. and Belward, A.S., 1992. The best index slope extraction (BISE): A method for reducing noise in NDVI time series. *Int. J. Rem. Sensing*, Vol:13, 8:1585-1590.
- Walter-Shea, E.A., Privette, J., Cornell, D., Mesarch, M.A., Hays, C.J., 1997, Relationship between directional spectral vegetation indices and leaf area and absorbed radiation in alfalfa. *Remote Sens. Environ.* (In press)
- Walthall, C.L., Norman, J.M., Welles, J.M., Campbell, G., and Blad, B.L., 1985, Simple equation to approximate the bi-directional reflectance from vegetative canopies and bare soil surfaces," *Applied Optics*, 24(3), pp. 383-

387.

Wanner W., A.H. Strahler, B. Hu, P. Lewis, J.-P. Muller, X. Li, C.L. Barker Schaaf, and M.J. Barnsley, 1997. Global retrieval of bidirectional reflectance and albedo over land from EOS MODIS and MISR data: Theory and algorithm. *J. Geoph. Res.*, 102, D14, 17143-17161.

Wanner W., X. Li, A.H. Strahler, 1995. On the Derivation of kernel-driven models of bidirectional reflectance. *J. Geoph. Res.*, 100, D10, 21077-21089

Wolfe. R., D. Roy. Georegistration of MODIS data (level 2G), to be submitted

Wu, A., Li, Z. and Cihlar, 1995, Effects of land cover type and greenness on advanced very high resolution radiometer bidirectional reflectances: Analysis and removal. *J. Geophys. Res.*, 100(D5), 9179-9192.